Electronic Supplementary Material (ESI) for Metallomics.


**Electronic Supplementary Information**

Wofford *et al*. "Ferric ions accumulate in the walls of dormant *Saccharomyces cerevisiae* cells and are reductively mobilized during reactivation"

Contents:

Table S1. Media composition.

| Abbreviations | Compositions |
|---|---|
| $^{57}Fe_{40}B_0$ | Synthetic minimal medium supplemented with $^{57}Fe$. *See* Ref (25). |
| $^{57}Fe_1B_{21}$ | MM (w/o Fe) + 1 μM $^{57}Fe$ + 21 μM BPS (bathophenanthroline disulfonate) |
| $Fe_0B_{30}$ | MM (w/o Fe) + 30 μM BPS |
| $Fe_0B_{100}$ | MM (w/o Fe) + 100 μM BPS |
| $Fe_0B_{100}$-NAB | MM (w/o Fe, w/o amino acids and bases) + 100 μM BPS |
| $^{56}Fe_{40}B_0$ | MM (w/o Fe) + 40 μM $^{56}Fe$ |
| $Fe_0B_0$ | MM (w/o Fe) |
| DW | Sterile deionized water |

Table S2. Final $OD_{600}$ and final Fe concentration of cells harvested during media switch experiments.

| Corresponding figures | Growth conditions | Final $OD_{600}$ | Final $[Fe]_{cell}$ (μM) |
|---|---|---|---|
| Figure 8A (before media switch) | Grown on $^{57}Fe_{40}B_0$ for 5 days | - | 4100 ± 400 |
| Figure 8A (before media switch) | Grown on $^{57}Fe_1B_{21}$ for 15 hours | - | 130 ± 20 |
| Figure 8A, filled circles | Grown on $^{57}Fe_{40}B_0$ for 5 days, switched to $Fe_0B_{30}$ at $OD_{Initial}$ = 0.01, grown for 4 days | 1.6 ± 0.3 | 57 ± 7 |
| Figure 8A, blank circles | Grown on $^{57}Fe_1B_{21}$ for 15 hours, switched to $Fe_0B_{30}$ at $OD_{Initial}$ = 0.01, grown for 4 days | 0.76 ± 0.39 | 23 ± 2 |
| Figure 8A, filled triangles | Grown on $^{57}Fe_{40}B_0$ for 5 days, switched to $Fe_0B_{100}$ at $OD_{Initial}$ = 0.01, grown for 5 days | 0.79 ± 0.15 | 110 ± 10 |
| Figure 8A, blank triangles | Grown on $^{57}Fe_1B_{21}$ for 5 days, switched to $Fe_0B_{100}$ at $OD_{Initial}$ = 0.01, grown for 5 days | 0.05 ± 0.02 | - |
| Figure 8B (before media switch) | Grown on $^{57}Fe_{40}B_0$ for 5 days | 1.7 ± 0.1 | 4900 ± 1500 |
| Figure 8B, filled squares | Grown on $^{57}Fe_{40}B_0$ for 5 days, switched to $^{57}Fe_{40}B_0$ at a conserved OD, grown for 1 day | 3.6 ± 0.5 | 3900 ± 900 |
| Figure 8B, blank squares | Grown on $^{57}Fe_{40}B_0$ for 5 days, switched to $Fe_0B_{100}$ at a conserved OD, grown for 1 day | 3.5 ± 0.2 | 1300 ± 400 |
| Figure 8B, crosses | Grown on $^{57}Fe_{40}B_0$ for 5 days, switched to $Fe_0B_{100}$-NAB at a conserved OD, grown for 1 day | 1.9 ± 0.1 | 2900 ± 900 |
| Figure 8C (before media switch) | Grown on $^{57}Fe_{40}B_0$ for 5 days | 2.2 ± 0.1 | 3900 ± 700<br>$[^{57}Fe]$ = 3800 ± 700 |

| | | | |
|---|---|---|---|
| Figure 8C, filled squares | Grown on $^{57}Fe_{40}B_0$ for 5 days, switched to $^{56}Fe_{40}B_0$ at a conserved OD, grown for 1 day | 4.2 ± 0.1 | 3100 ± 200<br>[$^{57}$Fe] = 860 ± 120 |
| Figure 8C, blank squares | Grown on $^{57}Fe_{40}B_0$ for 5 days, switched to $Fe_0B_{100}$ at a conserved OD, grown for 1 day | 4.2 ± 0.1 | 1500 ± 200 |
| Figure 8C, filled diamonds | Grown on $^{57}Fe_{40}B_0$ for 5 days, switched to 0Fe at a conserved OD, grown for 1 day | 4.2 ± 0.1 | 1200 ± 200 |
| Figure 8C, blank diamonds | Grown on $^{57}Fe_{40}B_0$ for 5 days, switched to DW at a conserved OD, grown for 1 day | 2.2 ± 0.2 | 2100 ± 500 |
| Figure 9A | Grown on $^{57}Fe_{40}B_0$ for 5 days | 1.7 | 3400 |
| Figure 9B | Grown on $^{57}Fe_{40}B_0$ for 5 days, switched to $Fe_0B_{100}$ at a conserved OD, grown for 1 day | 4.1 | 900 |
| Figure 9D | Grown on $^{57}Fe_{40}B_0$ for 5 days, switched to $Fe_0B_{100}$ at a conserved OD, grown for 1 day | 1.9 | 2000 |

**Appendix A. RMSD considerations**

In some experiments, data are not collected at equal time intervals (e.g. see $[O_2]$ trace in Figure 3). This situation distorts the process of model optimization because weighting each point equally favors better fits to the crowded regions of data at the expense of the fits to the sparse regions. But sparse regions may contain critical behavior that researchers might want to model. We wanted our simulated plots to weigh all time-intervals of such traces equally despite the unequal distribution of data. This required that we weigh sparse data more heavily than dense data. We used the following approach to do this.

Consider a 2D plot in which $n$ points are *unevenly* spaced in time, with the first point at $t_1 = 0$ and the last point $t_n$ at the end of the experiment. Let intermediate points $IP_{i,i+1}$ be equidistant between points $t_i$ and $t_{i+1}$ such that $IP_{i,i+1} = \left(t_i + t_{i+1}\right)/2$. Intermediate line segments $LS_i = IP_{i,i+1} - IP_{i-1,i} = (t_{i+1} - t_{i-1})/2$. The line segments for the initial and final points, $LS_1$ and $LS_n$ equal $t_2/2$ and $(t_n - t_{n-1})/2$, respectively. Then $t_n = \sum_{i=1}^{n} LS_i$. For each data point, the normalized weighting factors $wf_i = LS_i / t_n$.

The RMSD function used to optimize the fits of simulations to experimental traces was constructed by adding the contributions of the two traces generated in the experiment (OD and $O_2$). In the OD trace, 18 data points were collected whereas 30 data points were collected in the $O_2$ trace. Weighting each trace equally required multiplying the RMSD contributions due to the OD trace by a factor of 30/18. The final RMSD used to optimize the model was

$$RMSD = \frac{1}{60}\left[\begin{array}{l} \frac{30}{18}\left(\frac{t_{OD,2}}{2t_{OD,18}}\right)\frac{\left|[S]_{OD,1}-[D]_{OD,1}\right|}{[D]_{OD,1}} + \sum_{i=2}^{18}\frac{30}{18}\left(\frac{t_{OD,i+1}-t_{OD,i-1}}{2t_{OD,18}}\right)\frac{\left|[S]_{OD,i}-[D]_{OD,i}\right|}{[D]_{OD,i}} + \frac{30}{18}\left(\frac{t_{OD,18}-t_{OD,17}}{2t_{OD,18}}\right)\frac{\left|[S]_{OD,18}-[D]_{OD,18}\right|}{[D]_{OD,18}} \\ + \left(\frac{t_{O2,2}}{2t_{O2,18}}\right)\frac{\left|[S]_{O2,1}-[D]_{O2,1}\right|}{[D]_{O2,1}} + \sum_{j=2}^{30}\left(\frac{t_{O2,j+1}-t_{O2,j-1}}{2t_{O2,30}}\right)\frac{\left|[S]_{O2,j}-[D]_{O2,j}\right|}{[D]_{O2,j}} + \left(\frac{t_{O2,30}-t_{O2,29}}{2t_{O2,30}}\right)\frac{\left|[S]_{O2,30}-[D]_{O2,30}\right|}{[D]_{O2,30}} \end{array}\right]$$

**Appendix B: Propagation of iron concentrations with divisions**

The iron concentration for the first generation of cells and the isotopic ratio were measured. These give the relationships

$$[Fe_{cell}]_1 = [^{57}Fe]_1 + [^{56}Fe]_1 = 130$$

*also*

$$[^{56}Fe]_1 / [^{57}Fe]_1 = 1.1$$

*solving...*

$$[^{56}Fe]_1 = 68.1$$

$$[^{57}Fe]_1 = 61.9$$

Assume that X μM $^{56}$Fe and Y μM $^{57}$Fe from the environment enter the cells in association with each growth and division cycle. The $^{56}$Fe is presumed to arise from endogenous Fe in the medium whereas $^{57}$Fe is presumed to arise from Fe exported from the cell. For the second generation

$$[Fe_{cell}]_2 = [^{56}Fe]_2 + [^{57}Fe]_2 = \frac{[^{56}Fe]_1 + X}{2} + \frac{[^{57}Fe]_1 + Y}{2}$$

*also*

$$\frac{[^{56}Fe]_2}{[^{57}Fe]_2} = \frac{\frac{[^{56}Fe]_1 + X}{2}}{\frac{[^{57}Fe]_1 + Y}{2}}$$

For the third generation

$$[^{56}Fe]_2 = \frac{\frac{[^{56}Fe]_1 + X}{2} + X}{2} = \frac{[^{56}Fe]_1}{4} + \frac{X}{4} + \frac{X}{2}$$

$$[^{57}Fe]_2 = \frac{\frac{[^{56}Fe]_1 + Y}{2} + Y}{2} = \frac{[^{56}Fe]_1}{4} + \frac{Y}{4} + \frac{Y}{2}$$

For the seventh generation…

$$[^{56}Fe]_2 = \frac{[^{56}Fe]_1}{64} + \frac{X}{64} + \frac{X}{32} + \frac{X}{16} + \frac{X}{8} + \frac{X}{4} + \frac{X}{2} = \frac{[^{56}Fe]_1}{64} + \frac{63X}{64}$$

$$[^{57}Fe]_2 = \frac{[^{57}Fe]_1}{64} + \frac{63Y}{64}$$

$$[Fe_{cell}]_7 = \frac{[^{56}Fe]_1}{64} + \frac{63X}{64} + \frac{[^{57}Fe]_1}{64} + \frac{63Y}{64} = 23$$

*also*

$$\frac{[^{56}Fe]_7}{[^{57}Fe]_7} = \frac{\frac{[^{56}Fe]_1}{64} + \frac{63X}{64}}{\frac{[^{57}Fe]_1}{64} + \frac{63Y}{64}} = 4.4$$

Solving gives

$$[^{56}Fe]_7 = 18$$

$$[^{57}Fe]_7 = 3.3$$

**Table S3. Mössbauer Spectral Decompositions.** Parameters are the average obtained from the considered spectra; particular parameters are listed separately if they were significantly different. *Percentages of signals with broad range of A values (Fe aggregates) were estimated based on the intensity remaining after subtracting all assignable signals from original spectra. Bold-styled parameters were fixed when simulated. Symbols /1D or /5D indicates growth for 1 or 5 days, respectively. Arrows indicate transfer from one medium to another.

| Spectrum (**Total [Fe]**) | NHHS $Fe^{III}$ | NHHS $Fe^{II}$ | HS heme $Fe^{II}$ (and $[Fe_2S_2]^{2+}$) | Central Doublet (LS heme $Fe^{II}$ and $[Fe_4S_4]^{2+}$) | $Fe^{III}$ nano-particle (and broad feature*) | $Fe^{II}(BPS)_3$ |
|---|---|---|---|---|---|---|
| $A_{iso}/g_n\beta_n$ (kG) | -227 to -235 | - | - | **-** | - | - |
| $\delta$ (mm/s) | 0.5 – 0.6 | 1.34 ± 0.05 | 0.85 ± 0.03 | **0.45** | 0.53 ± 0.01 | 0.38 ± 0.01 |
| $\Delta E_Q$ (mm/s) | -1 to 0 | 3.06 ± 0.05 | 2.38 ± 0.07 | **1.15** | 0.52 ± 0.04 | 0.31 ± 0.01 |
| $\Gamma$ (mm/s) | 0.80 – 0.85 | 0.65 ± 0.07 | 0.39 ± 0.10 | **0.60** | 0.45 ± 0.10 | 0.32 ± 0.02 |
| Fig. 9A $^{57}Fe_{40}B_0$/5D **(3400 µM)** | 65% | 3% | - | - | 10% (20%) | - |
| Fig. 9B $^{57}Fe_{40}B_0$/5D → $Fe_0B_{100}$/1D | 27% | 10% | - | - | - | 60% |

| | | | | | | |
|---|---|---|---|---|---|---|
| **(900 µM)** | | | | | | |
| Fig. 9C 2B-minus-$FeBPS_3$ **(360 µM)** | 68% | 26% | 3% | 3% | - | - |
| Fig. 9D $^{57}Fe_{40}B_0$/5D → $Fe_0B_{100}$-NAB/1D **(2000 µM)** | 24% | 10% (1.3/3.0) 16% (1.1/3.8) | - | - | - | 48% |
| Fig. 9E 2D-minus-$FeBPS_3$ **(1000 µM)** | 48% | 20% (1.3/3.0) 30% (1.1/3.8) | - | - | - | - |
| Fig. 11A $^{57}Fe_{40}B_0$/5D **(5200 µM)** | 58% | 3% | - | - | 20% (17%) | - |
| Fig. 11B $^{57}Fe_{40}B_0$/5D → $Fe_0B_0$/1D **(1600 µM)** | 79% | 8% | 3% | 7% | 3% | - |
| Fig. 11C $^{57}Fe_{40}B_0$/5D | 63% | - | - | - | 28% (6%) | - |

| | | | | | | |
|---|---|---|---|---|---|---|
| → DW/1D **(3000 µM)** | | | | | | |
| Fig. 11D $^{57}Fe_{40}B_0$/5D → $Fe_0B_{100}$/1D **(1700 µM)** | - | - | - | - | - | > 90% |
| Fig. 11E $^{57}Fe_{40}B_0$/5D → $Fe_0B_{100}$/1D / Tris-washed **(160 µM)** | 32% | 20% | 6% | 27% | - | 15% |
| Fig. 11F $^{57}Fe_{40}B_0$/5D → $^{56}Fe_{40}B_0$/1D **(2900 µM, [$^{57}$Fe] = 710 µM)** | 46% | 12% | 3% | 3% | 36% | - |
| Fig. 12A $^{57}Fe_{40}B_0$/5D **(4500 µM)** | 48% | 2% | - | - | 20% (27%) | - |
| Fig. 12B $^{57}Fe_{40}B_0$/5D → | 43% | 6% | - | - | 23% (25%) | - |

| | | | | | | |
|---|---|---|---|---|---|---|
| $Fe_0B_{100}$/0.5 hr **(3600 µM)** | | | | | | |
| Fig. 12C $^{57}Fe_{40}B_0$/5D → $Fe_0B_{100}$/3 hr **(3100 µM)** | 45% | 4% | - | - | 20% (7%) | 22% |
| Fig. 12D $^{57}Fe_{40}B_0$/5D → $Fe_0B_{100}$/6 hr **(2700 µM)** | 38% | 2% | - | - | 6% (4%) | 48% |

**Figure S1. UV-Vis spectra of $Fe^{II}(BPS)_3$ solution and whole yeast cells.** A, 50 μM Fe-citrate and 150 μM BPS mixed in 100 mM Tris-HCl buffer (pH 9.4); B, 1 day-old cells grown on $Fe_{40}B_0$ medium were transferred to $Fe_0B_{100}$ medium (10-fold diluted in water); C, same as B, but rinsed with 100 mM Tris-HCl buffer (pH 9.4); D, rinses collected from C.

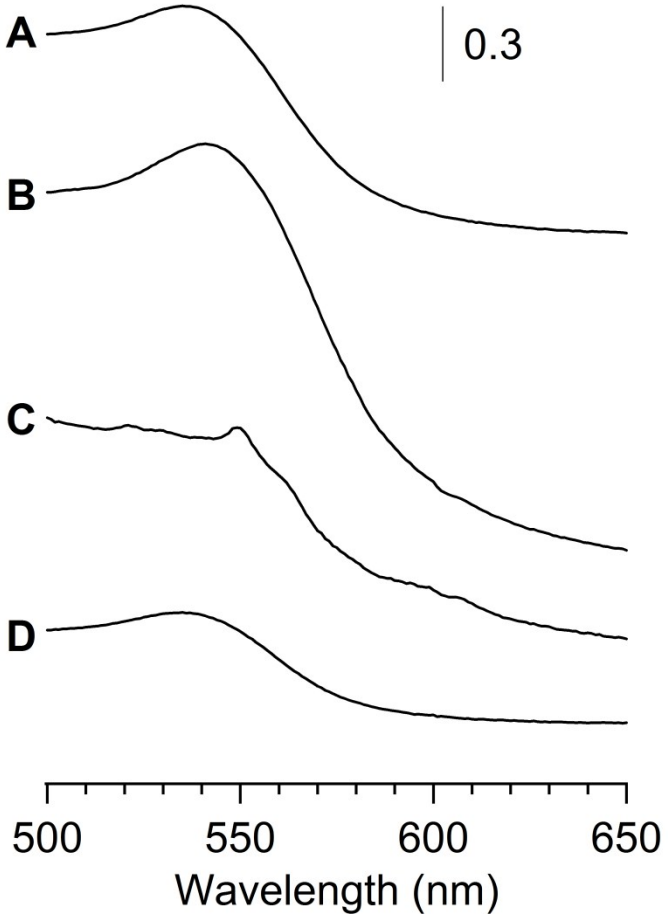

**Figure S2. Changes in percentages of Fe species found in Mössbauer spectra of $^{57}Fe_{40}B_0$ cells** transferred to $Fe_0B_{100}$ medium and harvested at 0.5, 3, 6 and 24 hr after the transfer. Open squares, NHHS $Fe^{III}$; solid squares, $Fe^{III}$ nanoparticles; pink circles, $Fe^{II}(BPS)_3$ complexes; blue circles, NHHS $Fe^{II}$. Spectral intensities at 24 hours after the medium transfer step were assumed to equal those of Figure 9D. Percentages at 0.5, 3, and 6 hr were obtained from Figure 12 B, C, and D. Percentages at 24 hr were obtained from Figure 11D.